

REACTION ZONES IN A FeSi75 FURNACE – RESULTS FROM AN INDUSTRIAL EXCAVATION

G. Tranel¹, M. Andersson², E. Ringdalen³, O. Ostrovski⁴ and J. J. Steinmo⁵

¹Department of Materials Science and Engineering, NTNU, Norway

²Luleå University of Technology, Sweden

³SINTEF Materials and Chemistry, Norway

⁴The University of New South Wales, Australia,

⁵Finnfjord AS

ABSTRACT

The paper presents results of an examination of the interior of a ferrosilicon furnace at Finnfjord, Norway, producing FeSi75. After tapping metal from the furnace, power was switched-off, while electrodes were left in their operating position. When the furnace had cooled down, a systematic core drilling and excavation of the furnace interior were carried out.

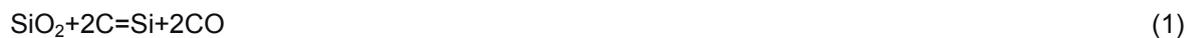
The core drilling was executed on a furnace cross-section to capture reaction zones across one of the electrodes and taphole and between the other two electrodes.

The excavation revealed a thick SiC slab on the furnace floor which obstructed tapping off the metal at the end of the furnace campaign. The crater wall was mainly formed from silicon carbide. A sintered mass of silicon carbide with partly molten silica was observed under the electrodes. Ferrosilicon was accumulated on the furnace floor which was covered by silicon carbide.

Samples taken from different reaction zones were characterised and analysed by optical microscopy, EPMA and XRD. Based on these observations and results, as well as prior work at NTNU/SINTEF, development of the reaction zones and metal forming mechanisms are discussed.

1 INTRODUCTION

The production processes for high-silicon ferrosilicon alloy and metallurgical silicon (MG-Si) are in principle very similar and primarily involve the reduction of silicon dioxide with carbon in an electric arc furnace. The main difference in the ferrosilicon process is that iron ore is added to the charge. The production of silicon can be described by the overall reaction:



Reactions in the furnace are, however, more complex and generally schematically classified into taking place in either the hot ($T > 1811^\circ\text{C}$), lower part of the furnace or the less hot ($T < 1512^\circ\text{C}$) upper part of the furnace⁽¹⁾. Hot zone reactions involve the production of silicon metal, in addition to SiO and CO gases according to:



SiO gas is carried by CO gas and recovered in the upper part of furnace through condensation or reactions forming silicon carbide:



The reduction of iron oxide to metallic iron takes place in the upper furnace zone, primarily through reactions with CO and volatiles produced in the lower part of the furnace. Carbon-saturated iron droplets in the furnace may also dissolve silicon through reactions with SiO gas according to:



From previously published results of pilot scale FeSi/Si furnace experiments and excavations⁽²⁻⁵⁾, a general picture of the reaction zones in the furnace has been obtained. In order to shed some further light on the reaction zones, metal forming reactions and gas transport paths involved in industrial FeSi production, a FeSi75 furnace at the Finnfjord plant in Norway, was cooled down/frozen during a normal production cycle. The furnace was subsequently carefully core drilled and excavated to reveal the state of raw materials and products at the time of shut down. The aim of the present paper is to illustrate the reaction zones and phases found in the furnace. Special emphasis is placed on formation and reactions in the arc crater wall, as well those reactions producing FeSi/Si metal.

2 The Furnace – Operation, Charge and Excavation

The Finnfjord plant in Finnsnes, northern Norway, produces approximately 100.000 tons of FeSi75 alloy annually in three furnaces using quartzite from Norway, iron ore pellets from Russia and Sweden, and coke and coal from China and North America.

Due to scheduled maintenance and the current market situation, the smallest of the three furnaces – furnace 1- was stopped during normal operation in November 2008. At the time, the furnace operated at 70 kA and 17,5 MW. The power was cut off and the furnace stopped with the electrodes down in operating position. The taphole was opened for 45 minutes and 1,73 tons of metal tapped before the furnace was allowed to cool naturally. After the furnace was stopped, the charge materials at the top were stoked to get an even surface. The surface in the centre of the furnace caved down approximately 530 mm during cooling of the furnace.

In April 2009, core drilling and excavation of the furnace was carried out by staff from Finnfjord, NTNU and SINTEF with assistance from Geo Drilling AS. The core drilling was carried out first to assure the position of materials before the excavation took place. Prior to the drilling, the loosely packed burden of the charge surface was poured with epoxy to bind the material together. The furnace was core-drilled in a cross section located between electrodes one and three, through the centre of electrode two, as illustrated in Figure 1.

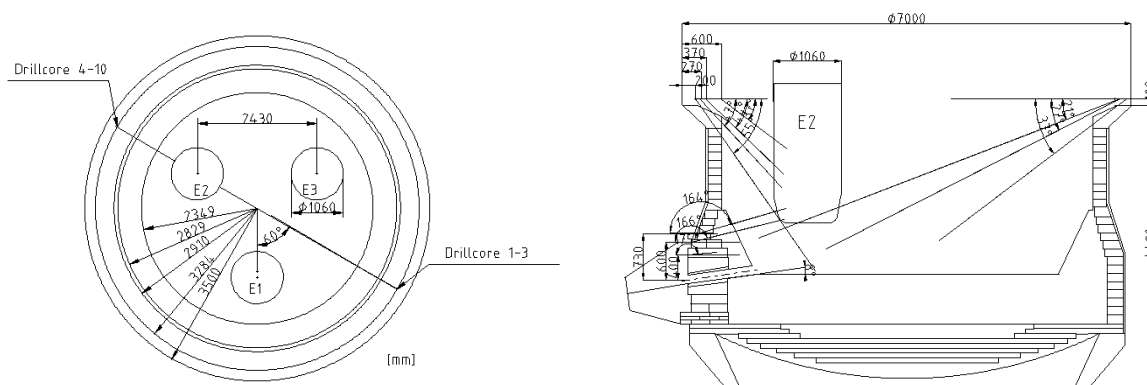


Figure 1. Geometry and core drilling pattern of the Finnfjord No. 1 furnace (all measurements in mm).

A total of 10 drill cores were taken from the top of the furnace at the edge of the flange with declining angles and from the mantle side at a location above the taphole.

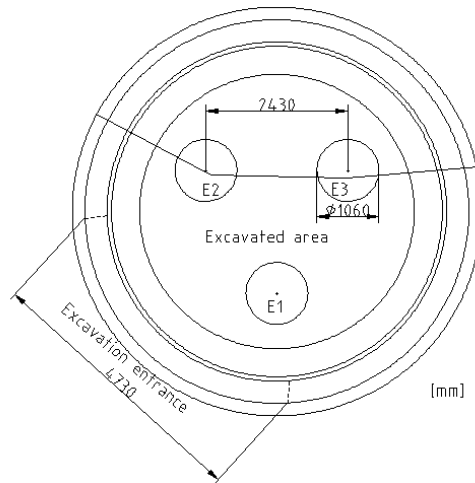


Figure 2: Excavated volume of Finnjord furnace

The excavated volume of the furnace (i.e. the volume where material was sampled) is illustrated in figure 2. The excavation entry (marked in the figure) was made by removing the steel mantle and the refractories in front of a taphole located between electrodes 1 and 2.

3 Observations, Analysis and Discussion of Phases in the Furnace

From the core drilling and excavation observations, an overview of reaction zones in the furnace is depicted in Figure 3.

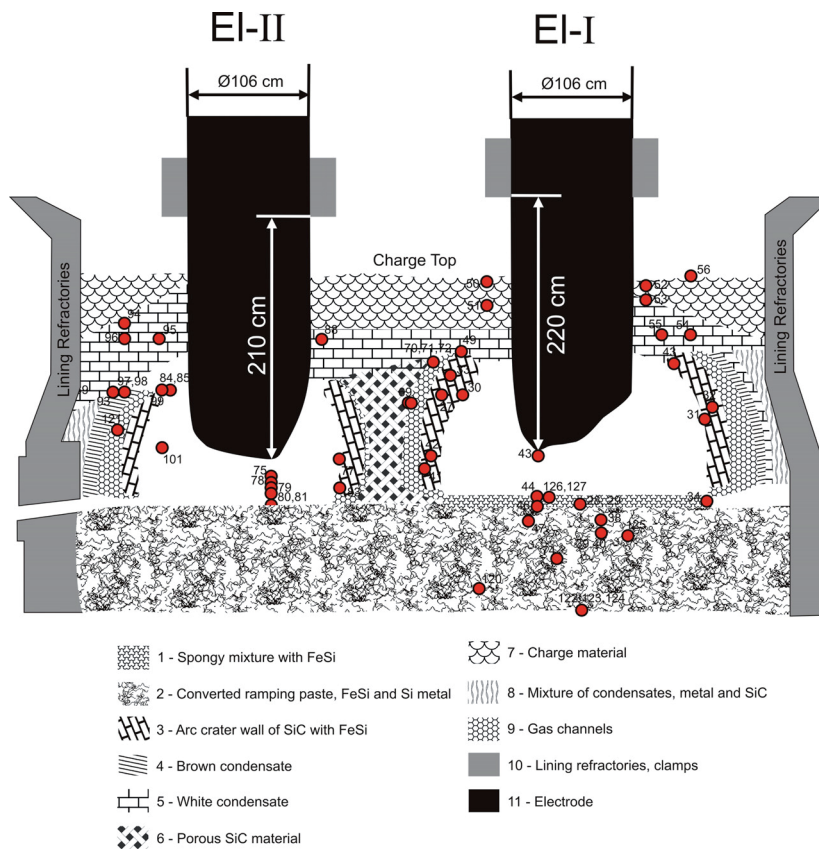


Figure 3: Overview of zones in the furnace around electrode 1. Dots represent sampling positions.

3.1 General observations

Raw materials on the top of the furnace were loosely packed and appeared not notably transformed in the top 200-300 mm of the furnace charge. Below the top charge, an approximately 500 mm thick horizontal zone of partly reacted raw materials, held together with glassy condensates, was observed. Figure 4 is a macrograph of such material. XRD analysis of the condensate material showed the presence of Si, confirming the condensation reaction (6).

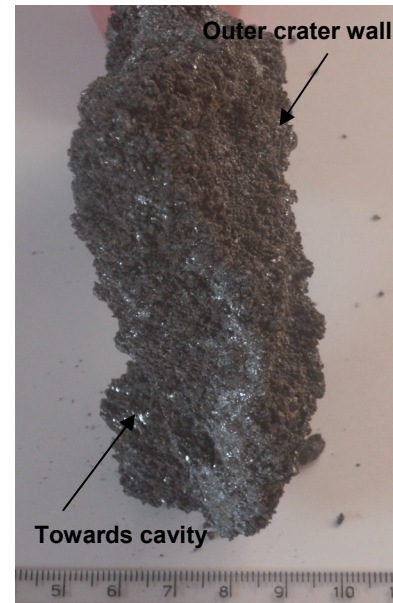


Figure 4: A typical sample of the material found in the “condensate zone”; partly reacted raw materials held together by white condensate

Figure 5: A typical layered crater wall macro-structure.

Intact crater walls around each of the three electrodes were found and determined as mainly built up of SiC and metal, with only a very limited content of quartz. These walls had a dense, layered structure, suggesting that the crater wall formation was a dynamic process, as seen in Figure 5. Crater walls extended up through the condensate layer and allowed large quantities of raw material charge falling / being transported along the electrode, down to the region below the electrode.

There were several gas channels on the outside of the crater walls, starting at the bottom of the crater. These channels were wider at the bottom of the crater (typically 200mm) and narrower at the top. The existence of such gas channels illustrate the strong gas flows also outside the crater, resulting from vigorous reactions under the electrode. Outside the gas channels and towards the furnace mantle, brown and white condensates were found in a layered structure, suggesting the presence of radial temperature zones in the furnace.

The material volumes outside the crater walls, towards the furnace walls, were characterised by vertical layers of different condensates. The charge outside the crater walls but towards the furnace centre - between the electrodes – consisted of a less dense bed of primarily silicon carbide (Figure 6).

Under the electrodes, heterogeneous mixtures of unreacted charge material (Figure 7) and reacted/molten raw materials were found. It was evident that charge material from the top of the furnace had fallen, probably during stoking, along the electrode down to the bath area under the electrode.

The excavation discovered metal at levels lower than the tap hole. The ramming paste at the base of the furnace reacted with silicon to form SiC and had vertical and horizontal “stripes” of metal intrusion below tap hole level. A metal layer was also found above the ramming paste. The metal layer below the tap hole increased in thickness from 400-1000 mm towards the centre of the furnace.



Figure 6: Loose charge between electrodes



Figure 7: "Unreacted" charge material from under electrode 1

The excavation revealed a thick SiC slab on the furnace floor which obstructed tapping off the metal at the end of the furnace campaign.

Representative samples from various zones of the furnace were selected and characterised primarily by Electron Microprobe Analysis (EPMA) and X-ray diffraction (XRD). Results from the investigations of samples from crater walls and under electrodes, are further detailed below.

3.2 Crater walls

Typical EPMA images of samples from the upper part of the crater wall towards the mantle around electrode 2 are illustrated in Figure 8 (a) and (b). These samples were taken 400mm from the charge top and 550 mm (a) or 250 mm (b) from the electrode respectively. The samples contained a silicon carbide phase, according to the analysis somewhat lower in carbon than the stoichiometric 1:1 ratio on atomic basis. Two distinct metallic carbon-saturated phases were found; one almost pure silicon phase and one phase with a composition close to $\text{Fe}_{45}\text{Si}_{55}$ on a weight basis. The later phase was likely precipitated from the liquid during cooling as predicted by the Fe-Si phase diagram⁶. Some small fractions of an Ca,Al,Si,Fe-oxide slag phase was also found, which originated from the ash content of the carbon materials and iron ore. In other samples taken from the upper part of the crater wall, very small amounts of a quartz-like phase were found in addition. The origin of silicon in this part, high up in the furnace, is not obvious Silicon may be generated from the condensation reaction [6]: $2\text{SiO}(\text{g})=\text{SiO}_2+\text{Si}$ at temperatures below 1811°C. However, SiO_2 in crater wall samples was found in a very small amount, what rises some doubts in this reaction. It may be more likely that temperature of the crater wall high up in the furnace, was high enough to make silicon formation possible according to the reaction:



It should be mentioned that the furnace operated with above the designed power what elevated temperature inside the furnace interior relative to the standard operation.

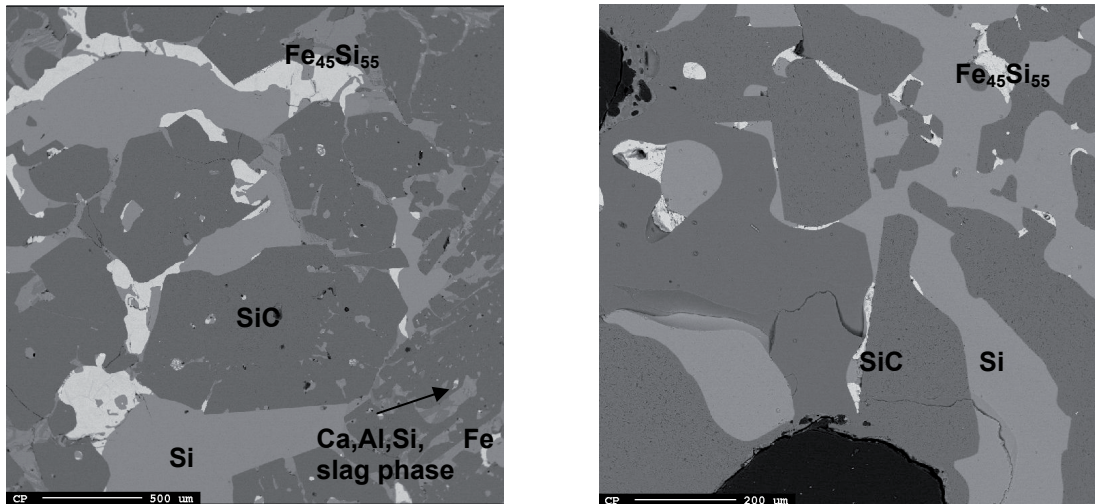


Figure 8(a) (left) and (b) (right): EPMA images of samples taken 400mm vertically from the charge top and 550 mm (a) or 250 mm (b) horizontally from the electrode respectively

The lower parts of the crater wall had many similarities with the upper parts. The presence of SiC, Si and Fe_xSi_y phases remain (Figure 9) although the wall density was higher. It is expected that the temperature was high enough in this zone for silicon to be produced by reaction (4). At the very bottom of the crater wall, interaction with the metal/slag bath was noted, and slag was found in the SiC-based crater wall (Figure 10).

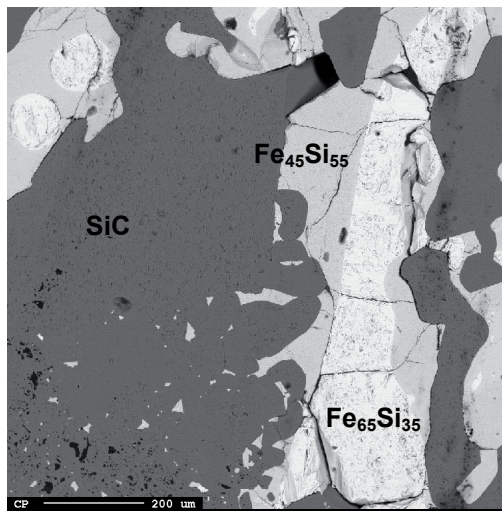


Figure 9: SiC and Fe_xSi_y phases in the lower part of the crater walls

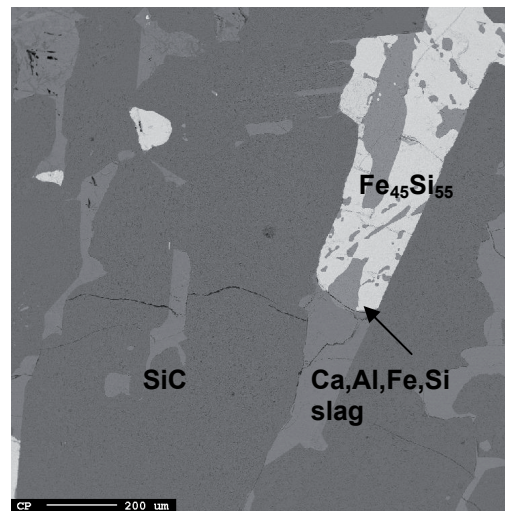


Figure 10: SiC, Fe_xSi_y and slag phases in the lower part of the crater walls

3.3 Under electrodes

Under the electrodes, a mixture of melted materials was found (Figure 11). Commonly, as seen in earlier excavations, the mixture contained melted quartz, SiC and alloy. The production of silicon in this zone is assumed to be primarily due to reaction between SiO and SiC (reaction (4)).

3.4 Metal bath

Under the mixture of melting raw materials, a bath of alloy was identified. The $Fe_{45}Si_{55}$ phase and SiC precipitated out during cooling (Figure 12).

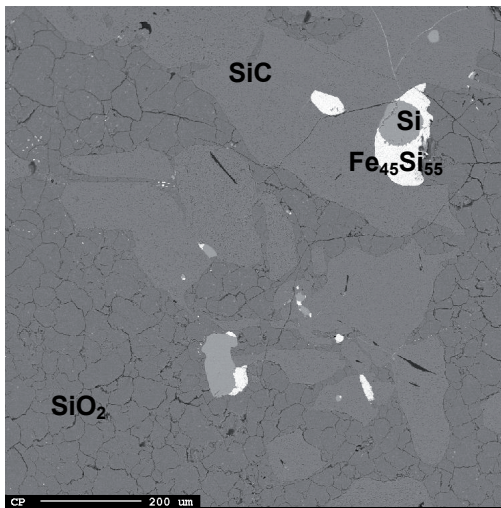


Figure 11: Material mix under electrodes

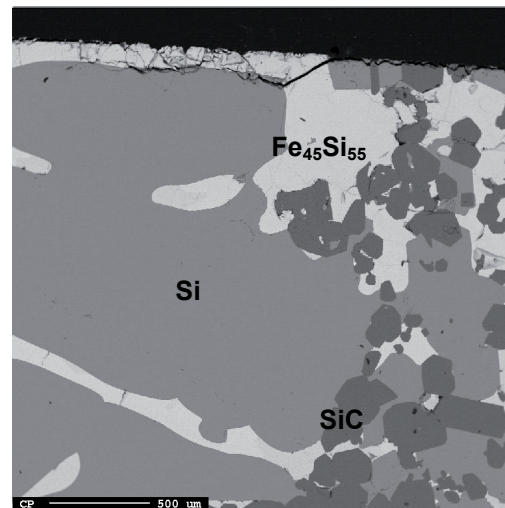


Figure 12: Phases in the metal bath under electrode 2

4 Summary and Conclusions

- An industrial scale FeSi75 furnace has been excavated for the purpose of mapping reaction zones and understanding metal forming reactions in the FeSi/Si process
- The arc crater walls contain primarily SiC, Si and Fe_xSi_y and in some instances SiO_2 .
- Production of silicon in the crater wall is most likely due to the reaction between SiC and SiO gas, according to the reaction: $\text{SiC(s)} + \text{SiO(g)} = 2\text{Si(s,l)} + \text{CO(g)}$. This appears to be the case also at the top part of the crater wall, high up in the furnace.
- The crater walls have a layered structure suggesting dynamic interactions between solid wall phases and gases.
- Deep gas channels on the outside of the crater walls suggest that significant gas transport takes place not only along the electrodes, but also along the outside of the crater walls up through the furnace.
- Transport of charge material from the top of the furnace takes place both along electrode and between electrodes.

5 Acknowledgements

The authors wish to thank the staff at Finnjord for excellent reception and organisation during the excavation in April 2009. We would also like to thank Johanna Salomonsson for preparing the EPMA samples, Morten Raanes for carrying out the analysis and Arjan Ciftja for drawing Figure 3. Financial support from the Norwegian ferroalloy producer's research association (FFF) and the Norwegian research council through the FUME project, is gratefully acknowledged.

6 References

1. Schei A., Tuset J.K., and Tveit, H. "Production of High Silicon Alloys". Tapir Forlag, Trondheim, Norway, 1998, ISBN: 8251913179
2. Myrhaug, E.H., "Non-fossil reduction materials in the silicon process – properties and behaviour", PhD thesis, NTNU, 2003.
3. Muller, M.B., Mellegaard, H.S., Lynum, H., and Olsen, S.E., "Electric reduction smelting. Reference experiment FeSi" (in Norwegian), SINTEF report, Trondheim, Norway, 1971.
4. Olsen, S.E. and Kristansen, J.O., "Production of 75%FeSi in pilot scale furnace" (In Norwegian), SINTEF Report STF34A73024, Trondheim, Norway, 1973.
5. Otani, Y., Saito, M., Usui, K and Chino, N. " The inner structure of submerged arc furnace" paper N.112, discussion M117D, 6th International Congress of Electroheat, Brighton, 1966.
6. Massalski, T.B., Baker, H., Bennet, L.H., Murray, L.J., "Binary Alloy Phase Diagrams", ASM International, 1986, ISBN: 0871702630

